nature geoscience

LETTERS

PUBLISHED ONLINE: 14 AUGUST 2011 | DOI: 10.1038/NGEO1219

Locally enhanced precipitation organized by planetary-scale waves on Titan

Jonathan L. Mitchell[1]*, Máté Ádámkovics[2], Rodrigo Caballero[3,4] and Elizabeth P. Turtle[5]

Saturn's moon Titan exhibits an active weather cycle that involves methane[1–8]. Equatorial and mid-latitude clouds can be organized into fascinating morphologies on scales exceeding 1,000 km (ref. 9). Observations include an arrow-shaped equatorial cloud that produced detectable surface accumulation, probably from the precipitation of liquid methane[10]. An analysis of an earlier cloud outburst indicated an interplay between high- and low-latitude cloud activity, mediated by planetary-scale atmospheric waves[11]. Here we present a combined analysis of cloud observations and simulations with a three-dimensional general circulation model of Titan's atmosphere, to obtain a physical interpretation of observed storms, their relation to atmosphere dynamics and their aggregate effect on surface erosion. We find that planetary-scale Kelvin waves arise naturally in our simulations, and robustly organize convection into chevron-shaped storms at the equator during the equinoctial season. A second and much slower wave mode organizes convection into southern-hemisphere streaks oriented in a northwest–southeast direction, similar to observations[9]. As a result of the phasing of these modes, precipitation rates can be as high as twenty times the local average in our simulations. We conclude that these events, which produce up to several centimetres of precipitation over length scales exceeding 1,000 km, play a crucial role in fluvial erosion of Titan's surface.

Titan's slow rotation (16 terrestrial days) and small radius (40% that of Earth) conspire to allow a global Hadley circulation, the tropical meridional overturning circulation of the atmosphere. As a result, Titan's strongest zonal winds are shifted polewards relative to Earth's, meridional temperature gradients are weak[12], and baroclinic cyclogenesis associated with storm-track weather is suppressed[13]. This dynamical configuration gives Titan an 'all tropics' climate[14]. Titan's intertropical convergence zone (ITCZ) migrates from one summer hemisphere to the other. Models predict a transient phase just following equinoxes when the ITCZ passes over the equator[14–16] and, during this time, Earth-like tropical disturbances would be expected at Titan's equator[9,17].

Classical shallow-water theory[18] predicts the existence of a broad spectrum of linear equatorial wave modes, including equatorially-trapped Rossby, Kelvin and mixed Rossby-gravity waves. All of these modes can be detected in Earth's atmosphere through spectral analysis of observations, which show power concentrated at planetary scales ($>10^4$ km; ref. 19). Through their surface convergence and induced vertical motion, the modes collectively organize the location and timing of clouds and precipitation in Earth's tropics on intraseasonal timescales. As a result of low insolation and a stabilizing antigreenhouse effect[20], moist convection on Titan cannot be maintained purely through surface evaporative fluxes, indicating that moisture convergence provided by large-scale modes of circulation is important for convective cloud formation[14,16,17,21,22].

Titan's methane clouds have received much attention since they were first discovered spectroscopically[1]. Although cloud-cover is spatially limited, large outbursts of cloud activity occasionally occur[23], as do cloud-free conditions[24]. Mesoscale clouds can remain stationary for days[22,25,26]. Titan's seasons progress slowly, taking roughly seven years to transition from solstice to equinox. The most recent northern spring equinox (NSE) occurred on 11 August 2009. Since that time, the location of cloud activity has shifted from southern (summer) mid- and high-latitudes to the equatorial region[9,26,27].

More recently, Cassini Imaging Science Subsystem (ISS) images of Titan have revealed large-scale clouds with an interesting array of morphologies and characteristics[9]. Most strikingly, an arrow-shaped cloud oriented eastwards was observed at the equator on 27 September 2010 (ref. 9), followed by observations of surface wetting which gradually diminished over several months[10]. We now use our fully three-dimensional Titan general circulation model (GCM) (described in Methods and Supplementary Information) to examine the dynamical origin of these storms, and we develop a methodology for comparing model precipitation rates to cloud observations.

Cloud opacity depends on the sizes and amount of suspended, condensed methane. Our Titan GCM has a moist convection scheme which predicts a surface precipitation rate, and we assume precipitation is associated with optically thick clouds. A small number of physically motivated assumptions (described in Methods and Supplementary Information) allow us to simulate cloud opacity in ISS bands using the GCM's precipitation field, thereby quantitatively linking cloud opacity to the amount of precipitation. Simulated observations of two events during the equinoctial transition of our GCM are shown in Fig. 1b,e. The two cloud events observed by Cassini ISS are shown in Fig. 1c,f: a cloud shaped like a chevron at the equator pointing eastwards was observed on 27 September 2010, followed on 18 October 2010 by a streak of clouds extending southeastwards from low-latitudes to high-latitudes[9]. Figure 1 demonstrates that our Titan GCM produces convective storms with the basic morphology of the two cloud observations. The dynamics underlying these storms are now examined through diagnostics of the GCM.

Figure 2 shows snapshots of the GCM simulation of Titan shortly following NSE. During this time, the ITCZ is passing over the equator and establishing itself in the northern hemisphere (Supplementary Fig. S7). Figure 2a,c shows the surface wind field with the zonal mean subtracted (arrows) and the 15-day

[1]Earth & Space Sciences, Atmospheric & Oceanic Sciences, University of California, Los Angeles, California 90095, USA, [2]Astronomy Department, University of California, Berkeley, California 94720, USA, [3]Department of Meteorology (MISU), Stockholm University, 106 91 Stockholm, Sweden, [4]Bert Bolin Centre for Climate Research, Stockholm University, 106 91 Stockholm, Sweden, [5]Johns Hopkins University, Applied Physics Laboratory, Laurel, Maryland 20723, USA. *e-mail: jonmitch@ucla.edu.

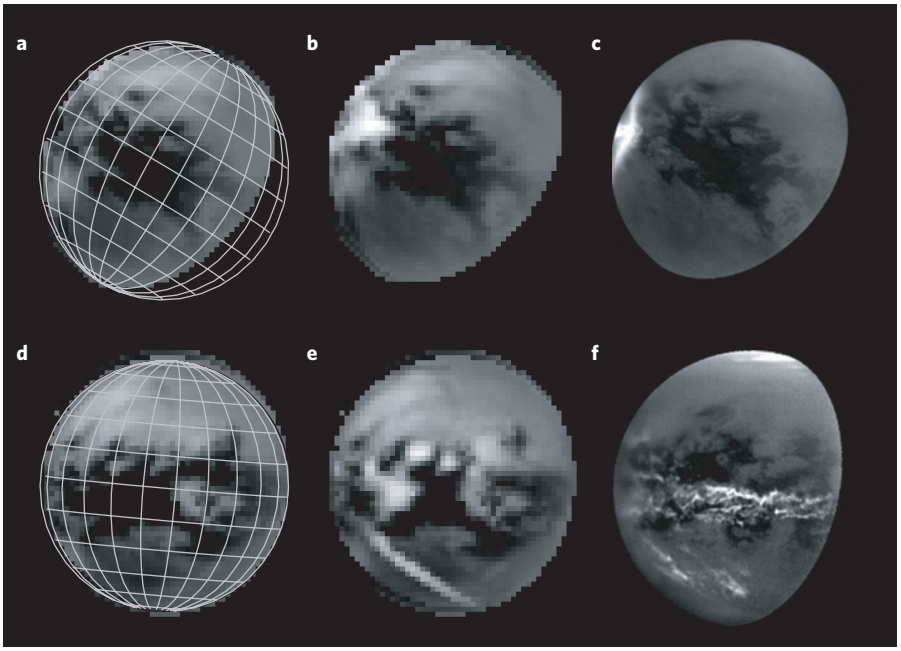

Figure 1 | Titan's clouds (right) are organized by planetary-scale waves that dominate storm activity in model simulations (centre). a,**d**, Simulations of cloud-free observations at 938 nm with lines of latitude and longitude used for comparison with models that include cloud opacity distributions (**b**,**e**) set by the precipitation from the GCM output as described in Methods (shown in Fig. 2). Viewing geometry and illumination angle are selected to reproduce Cassini observations[9] on 27 September 2010 (**c**) and 18 October 2010 (**f**). GCM models (**b**,**e**) are divided by a simulated 619 nm image to reproduce the image processing used for the observations. No parameter tuning is required to produce a similar contrast to observations, indicating a close correspondence between the modelled precipitation field and the observed clouds.

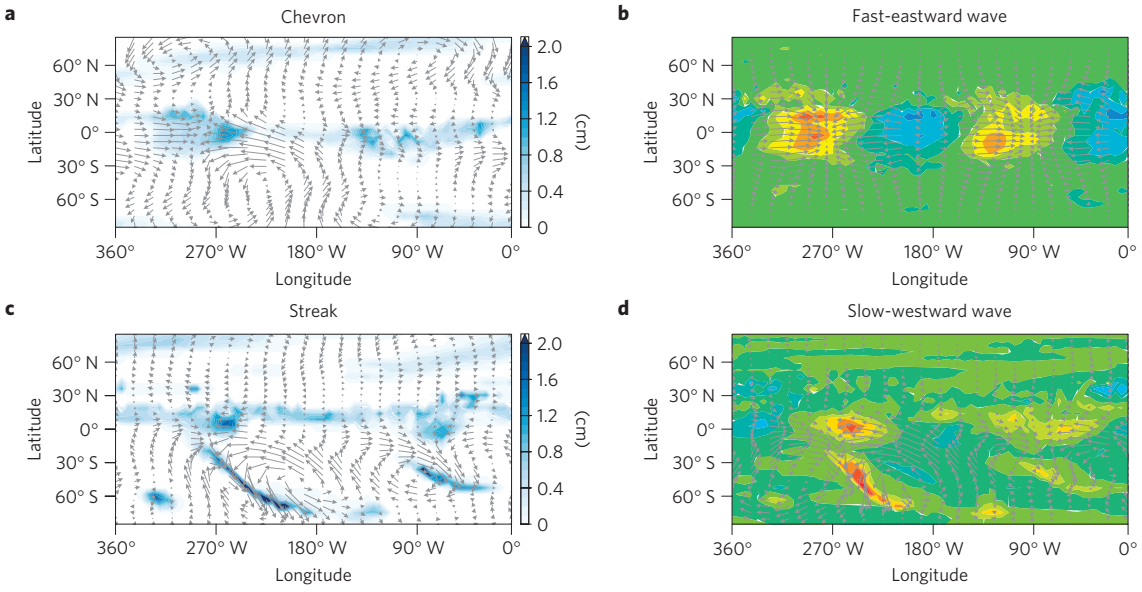

Figure 2 | Simulated precipitation and surface wind patterns in selected events during the equinoctial season (left column) and derived from statistical analysis (right column). a, Fifteen-terrestrial-day cumulative precipitation (blue, cm) and surface winds with the zonal mean subtracted (arrows) for an equatorial chevron-shaped event. **b**, Regression of the leading principal component associated with eastward-propagating variance (see Supplementary Information) onto the surface winds (arrows) and precipitation (colours). **c**, As in **a** but for a mid-latitude streak event. The length of wind vector arrows have been increased by a factor of three. **d**, As in **b** but for westward-propagating variance.

cumulative precipitation of the events shown in Fig. 1b,e (blue, cm). The cumulative precipitation of these storms indicates greatly enhanced precipitation rates compared with the global- and time-mean of less than 0.1 mm d^{-1}. Near the equator, zonally elongated bands of precipitation are being maintained by the circulation, marking the location of the ITCZ. Figure 2a clearly shows a chevron precipitation feature at longitude 260° W at the equator that is spatially coincident with a region of horizontal convergence of surface winds, indicating a role for gravity waves. The chevron produces one to two centimetres of precipitation over a 2,000-km-wide region during its lifetime, an amount sufficient to create runoff and erosion of the equatorial surface[28]. A few months of integration later, the model produces a precipitation and wind pattern extending from the equator deep into the southern

hemisphere, as seen in Fig. 2c. This streaking precipitation is produced by a combination of convergent and circulating surface winds, indicating a role for both gravity waves and Rossby waves. The depth of convection in the streaking feature is shallower than the chevron (Supplementary Fig. S6), however its lifetime is considerably longer, resulting in several centimetres of precipitation over its extent. Currently published ISS images do not show evidence for surface changes associated with the storm in Fig. 1f, which suggests these clouds do not produce substantial rainfall. This indicates that our model overestimates the amount of mid-latitude precipitation during the current season.

Precipitation rates within these modes exceed the zonal- and time-mean rate by a factor of ~20 during the equinoctial transition (Fig. 3a). We infer that three-dimensional dynamics are responsible for local and significant enhancements in precipitation, and are therefore essential for understanding the observed distribution of surface erosion[29]. Equatorial chevrons are ephemeral features of Titan's climate, however, occurring on the order of an Earth year as Titan's ITCZ undergoes a post-equinoctial transition from one hemisphere to the other (Supplementary Figs S7 and S10; ref. 17). Surface accumulation (that does not infiltrate into the regolith) evaporates away during the summer (Supplementary Fig. S8), with important implications for observed fluvial features in Titan's semi-arid environment[29].

We now show that the cloud structures in the examples above are not isolated occurrences, but instead constitute the 'typical' behaviour of convection in the model, organized by well-defined dynamical modes of the atmosphere. The evolution in time and longitude of modelled equatorial precipitation (Fig. 3a) shows evidence of eastward-propagating disturbances with a phase speed of about 12 m s^{-1} (indicated by the solid black line), superposed on slower disturbances travelling westwards at around 1 m s^{-1} (dashed line). These two modes of variability are also apparent in a space–time power spectrum of equatorial surface zonal wind (Fig. 3b), which shows sharp peaks at an eastward-propagating zonal wavenumber of 2 with a period of about eight days (corresponding to a phase speed of about 12 m s^{-1} at the equator) and at a westward-propagating zonal wavenumber of 2 with period ~ 100 days (phase speed ~ 1 m s^{-1}). This close correspondence between precipitation and surface wind perturbations implies a link between dynamical and convective processes, as seen in convectively coupled equatorial waves on Earth[19].

To isolate the spatial structure of the dominant eastward and westward modes, we follow a three-step procedure described in Methods. The spatial structure and phase speed of the eastward-propagating mode corresponds closely to that of a baroclinic, equatorially trapped Kelvin wave (see Supplementary Information). The spatial patterns of precipitation and surface wind anomaly of this mode are shown in Fig. 2c. Crucially, these waves are associated with roughly chevron-shaped equatorial precipitation patterns. The westward-propagating mode (Fig. 2d) stretches from the equator to the high-latitudes of the Southern Hemisphere, and is associated with a streak-like precipitation feature stretching southeastwards from the tropics into the mid-latitudes. Thus, convective storms in the GCM are organized by large-scale modes of variability, and the modes are robustly associated in a statistical sense with precipitation structures resembling the observed clouds.

We have also conducted sensitivity tests to investigate the feedback of moist convective heating onto the dynamical modes (see Supplementary Information for details). In a simulation where latent heating by convection and surface evaporation is artificially suppressed, we find that the eastward-propagating Kelvin mode is unchanged, whereas the westward mode is substantially altered (Fig. 3c). Thus the Kelvin mode is convectively uncoupled (see Supplementary Information), although its surface convergence field plays an important role in organizing precipitation. Convection

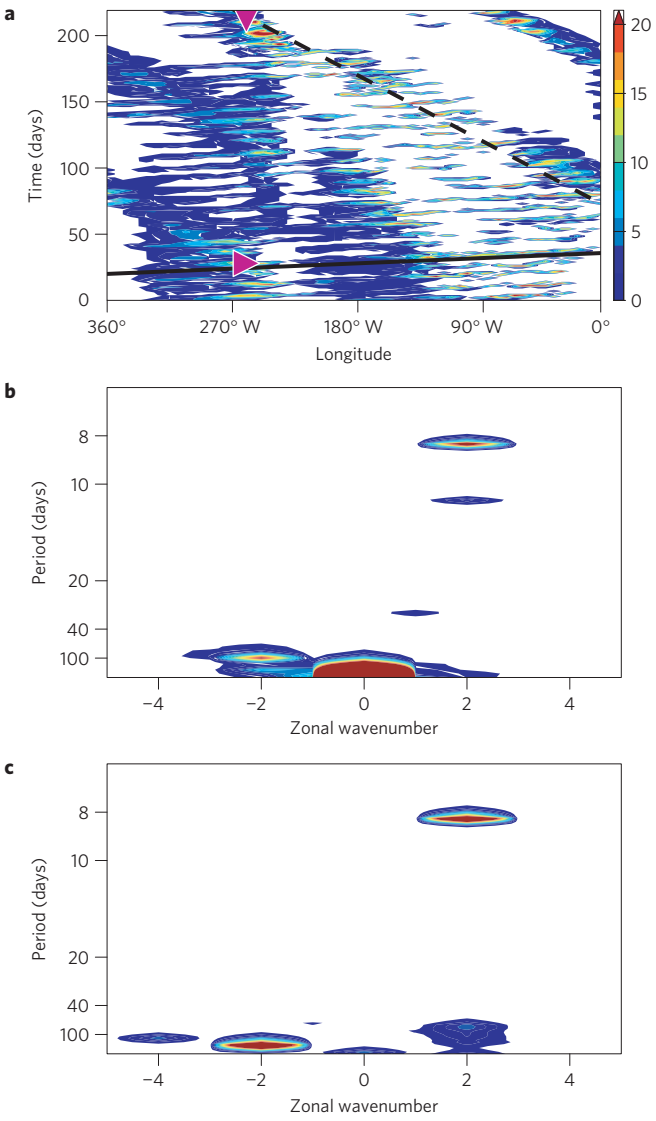

Figure 3 | Space–time variability of simulated equatorial winds and precipitation averaged over ±10° latitude in the Titan GCM. **a**, Longitude–time distribution of precipitation rate normalized to the global- and time-mean rate for the period containing the chevron event in Fig. 1 (magenta triangle at day 30) and the streak event (triangle at day 210). Lines indicate constant velocity trajectories of 11.7 m s^{-1} eastwards (solid) and 0.9 m s^{-1} westwards (dashed). **b**, Space–time spectral decomposition of surface zonal winds for 1,000 simulation days centred around the equinox. **c**, As in **b** but for a test simulation with the latent heating of methane removed.

is essential to the dynamics of the westward mode, however, as indicated by the substantial reduction of precipitation at negative wavenumbers in the test case (Fig. 3c; also see Supplementary Information). This is the first evidence of a convectively coupled wave on a planetary body other than Earth.

A sequence of cloud observations taken in 2008 (before NSE) with ground-based instruments indicated a connection between disturbances at equatorial and polar latitudes likely to be mediated by planetary-scale waves[11]. This cloud propagated eastwards at ~3 m s^{-1}, and was interpreted as a stationary Rossby wave advected by the mid-tropospheric wind. However, our simulation indicates that the eastward-propagating precipitation field during this epoch is associated with the Kelvin wave component. As this observation occurred before NSE, surface convergence resulting

from the superposition of the Kelvin mode and the ITCZ is most intense south of the equator (Supplementary Fig. S10). As the season transitions towards Northern Summer Solstice (NSS), our model indicates a shift in the precipitation by the Kelvin–ITCZ superposition to northern mid-latitudes accompanied by southern mid-latitude streaks. We therefore predict a phase of transient cloud activity in both hemispheres of Titan during the next several years (Supplementary Fig. S7).

In summary, we have developed a process for interpreting the morphologies of and precipitation associated with Titan's clouds through a combined analysis of observations and GCM simulations, thereby opening a new field of dynamic meteorology. We find that recent cloud activity near Titan's equator just following NSE is consistent with the presence of two dominant modes of atmospheric variability in the GCM. A fast, eastward-propagating mode travelling at $\sim$12 m s^{-1} with the character of an equatorially trapped Kelvin wave produces chevron-shaped precipitation patterns similar to the clouds observed by Cassini ISS on 27 September 2010 (ref. 9). A slow, westward-propagating mode that is vertically confined accounts for streaks of precipitation such as the cloud observed on 18 October 2010 (ref. 9). This latter mode is convectively coupled, the first of its kind to be inferred outside of Earth's atmosphere. The phasing of these modes produce several centimetres of precipitation over 1,000-km-scale regions, locally enhancing precipitation rates by 20-fold over the mean. These modes therefore play a crucial role in fluvial erosion of Titan's surface. Observations clearly indicate surface changes associated with the equatorial chevron[10], but precipitation from the mid-latitude streak is too light to be detected, indicating the model overestimates mid-latitude precipitation during the current season.

Methods

Our Titan GCM is similar to that used in a previous study[16], the primary difference being that the model is now fully three-dimensional. Simplified treatments of radiation, convection, and the seasonal cycle are included. The model does not include tides, either thermal (diurnal) or gravitational (semi-diurnal), nor any other non-axisymmetric forcing mechanism (be it topography, albedo, opacity sources, or others.). The atmosphere is spun up and moistened by methane evaporation from an initial state of solid-body rotation and zero methane humidity. The seasonal cycle of insolation is included in the model forcing; see the Supplementary Information for a more detailed description. A (statistical) steady state is achieved after $\sim$20 Titan years ($\sim$600 Earth years). The results shown in the figures are from 1,000 terrestrial days bracketing NSE of the 21st simulated Titan year. (The zonal- and time-mean overturning streamfunction, zonal winds, and temperature of the full, 1,800 model days are shown in the Supplementary Information.)

The GCM does not include a cloud scheme, so we have developed a method for simulating cloud observations based on precipitation. Briefly, we assume cloud droplets are distributed about a peak size of 512 µm, which are marginally lofted for convective updrafts of 10 m s^{-1}, typical for deep convective events on Titan[21]. We assume 10–20% of the column precipitation remains suspended, with a cloud-top altitude of 20 km. Together the column mass of the cloud and the droplet size distribution determine the cloud optical depth. Mie theory then translates the droplet size distribution into the scattering properties of clouds, ultimately linking the precipitation field from the GCM to the radiative transfer model (see Supplementary Information for more details).

To isolate the spatial structure of dominant modes of variability in the GCM, the surface zonal wind field is spectrally filtered to retain only the space and timescales of the dominant spectral peaks; the leading patterns of variability of the filtered surface wind are extracted using empirical orthogonal function (EOF) analysis, and the associated three-dimensional fields are reconstructed by regression onto the leading principal component; further details are given in the Supplementary Information.

Received 5 April 2011; accepted 1 July 2011; published online 14 August 2011

References

1. Griffith, C., Owen, T., Miller, G. & Geballe, T. Transient clouds in Titan's lower atmosphere. *Nature* **395,** 575–578 (1998).
2. Griffith, C., Hall, J. & Geballe, T. Detection of daily clouds on Titan. *Science* **290,** 509–513 (2000).
3. Tokano, T. *et al.* Methane drizzle on Titan. *Nature* **442,** 432–435 (2006).
4. Ádámkovics, M., Wong, M., Laver, C. & de Pater, I. Widespread morning drizzle on Titan. *Science* **318,** 962–965 (2007).
5. Brown, M., Smith, A., Chen, C. & Ádámkovics, M. Discovery of fog at the south pole of Titan. *Astrophys. J. Lett.* **706,** L110–L113 (2009).
6. Turtle, E. *et al.* Cassini imaging of Titan's high-latitude lakes, clouds, and south-polar surface changes. *Geophys. Res. Lett.* **36,** L02204 (2009).
7. Turtle, E., Perry, J., Hayes, A. & McEwen, A. Shoreline retreat at Titan's Ontario Lacus and Arrakis Planitia from Cassini Imaging Science Subsystem observations. *Icarus* **212,** 957–959 (2011).
8. Hayes, A. G. *et al.* Transient surface liquid in Titan's polar regions from Cassini. *Icarus* **211,** 655–671 (2011).
9. Turtle, E. *et al.* Seasonal changes in Titan's meteorology. *Geophys. Res. Lett.* **38,** L03203 (2011).
10. Turtle, E. *et al.* Rapid and extensive surface changes near Titan's equator: Evidence of April showers. *Science* **331,** 1414–1417 (2011).
11. Schaller, E., Roe, H., Schneider, T. & Brown, M. Storms in the tropics of Titan. *Nature* **460,** 873–875 (2009).
12. Achterberg, R., Conrath, B., Gierasch, P., Flasar, F. & Nixon, C. Titan's middle-atmospheric temperatures and dynamics observed by the Cassini Composite Infrared Spectrometer. *Icarus* **194,** 263–277 (2008).
13. Mitchell, J. & Vallis, G. The transition to superrotation in terrestrial atmospheres. *J. Geophys. Res.* **115,** E12008 (2010).
14. Mitchell, J., Pierrehumbert, R., Frierson, D. & Caballero, R. The dynamics behind Titan's methane clouds. *Proc. Natl Acad. Sci. USA* **103,** 18421–18426 (2006).
15. Tokano, T. Impact of seas/lakes on polar meteorology of Titan: Simulation by a coupled GCM-Sea model. *Icarus* **204,** 619–636 (2009).
16. Mitchell, J., Pierrehumbert, R., Frierson, D. & Caballero, R. The impact of methane thermodynamics on seasonal convection and circulation in a model Titan atmosphere. *Icarus* **203,** 250–264 (2009).
17. Mitchell, J. The drying of Titan's dunes: Titan's methane hydrology and its impact on atmospheric circulation. *J. Geophys. Res.* **113,** E08015 (2008).
18. Matsuno, T. Quasi-geostrophic motions in the equatorial area. *J. Meteor. Soc. Jpn* **44,** 25–42 (1966).
19. Wheeler, M. & Kiladis, G. Convectively coupled equatorial waves: Analysis of clouds and temperature in the wavenumber–frequency domain. *J. Atmos. Sci.* **56,** 374–399 (1999).
20. McKay, C., Pollack, J. & Courtin, R. The greenhouse and antigreenhouse effects on Titan. *Science* **253,** 1118–1121 (1991).
21. Barth, E. L. & Rafkin, S. C. R Convective cloud heights as a diagnostic for methane environment on Titan. *Icarus* **206,** 467–484 (2010).
22. Ádámkovics, M., Barnes, J., Hartung, M. & de Pater, I. Observations of a stationary mid-latitude cloud system on Titan. *Icarus* **208,** 868–877 (2010).
23. Schaller, E., Brown, M., Roe, H. & Bouchez, A. A large cloud outburst at Titan's south pole. *Icarus* **182,** 224–229 (2006).
24. Schaller, E., Brown, M., Roe, H., Bouchez, A. & Trujillo, C. Dissipation of Titan's south polar clouds. *Icarus* **184,** 517–523 (2006).
25. Roe, H., Brown, M., Schaller, E., Bouchez, A. & Trujillo, C. Geographic control of Titan's mid-latitude clouds. *Science* **310,** 477–479 (2005).
26. Rodriguez, S. *et al.* Global circulation as the main source of cloud activity on Titan. *Nature* **459,** 678–682 (2009).
27. Brown, M., Roberts, J. & Schaller, E. Clouds on Titan during the Cassini prime mission: A complete analysis of the VIMS data. *Icarus* **205,** 571–580 (2010).
28. Jaumann, R. *et al.* Fluvial erosion and post-erosional processes on Titan. *Icarus* **197,** 526–538 (2008).
29. Langhans, M. *et al.* Titan's fluvial valleys: Morphology, distribution, and spectral properties. *Planet. Space Sci.* http://dx.doi.org/10.1016/j.pss.2011.01.020 (in the press).

Acknowledgements

E.P.T. is supported by NASA's Cassini–Huygens mission.

Author contributions

J.L.M. contributed experiment design, performed GCM simulation analysis, and wrote the manuscript. M.Á. and J.L.M. developed the algorithm for simulating clouds from the GCM, and M.Á. contributed radiative transfer analysis of the GCM. R.C. contributed the statistical analysis of the GCM simulation and J.L.M. and R.C. interpreted the model dynamics. E.P.T. contributed analysis of Cassini ISS cloud images.

Additional information

The authors declare no competing financial interests. Supplementary information accompanies this paper on www.nature.com/naturegeoscience. Reprints and permissions information is available online at http://www.nature.com/reprints. Correspondence and requests for materials should be addressed to J.L.M.